Langmuir

Article

Hierarchical Assemblies of Gold Nanoparticles at the Surface of a Film Formed by a Bridged Silsesquioxane Containing Pendant Dodecyl Chains

Mari#a L. Go#mez, Cristina E. Hoppe, Ileana A. Zucchi, Roberto J. J. Williams, Marina I. Giannotti, and M. Arturo Lo#pez-Quintela

Langmuir, **2009**, 25 (2), 1210-1217 • DOI: 10.1021/la8033403 • Publication Date (Web): 23 December 2008

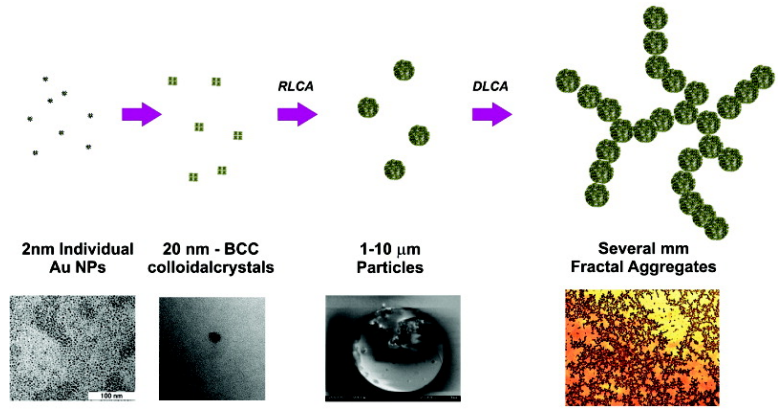

More About This Article

Additional resources and features associated with this article are available within the HTML version:

- Supporting Information
- Access to high resolution figures
- Links to articles and content related to this article
- Copyright permission to reproduce figures and/or text from this article

View the Full Text HTML

Hierarchical Assemblies of Gold Nanoparticles at the Surface of a Film Formed by a Bridged Silsesquioxane Containing Pendant Dodecyl Chains

María L. Gómez,[†] Cristina E. Hoppe,*[,†] Ileana A. Zucchi,[†] Roberto J. J. Williams,*[,†] Marina I. Giannotti,[‡] and M. Arturo López-Quintela[§]

Institute of Materials Science and Technology (INTEMA), University of Mar del Plata and National Research Council (CONICET), J. B. Justo 4302, 7600 Mar del Plata, Argentina, Networking Biomedical Research Center on Bioengineering, Biomaterials and Nanomedicine (CIBER-BBN) and Department of Physical Chemistry, University of Barcelona, Barcelona, Spain, and Laboratory of Magnetism and Nanotechnology, Department of Physical Chemistry, University of Santiago de Compostela, Santiago de Compostela, Spain

Received October 9, 2008. Revised Manuscript Received November 5, 2008

Hierarchical aggregates of gold nanoparticles (NPs) on different length scales were in situ generated at the surface of a bridged silsesquioxane during the process of film formation by polycondensation and solvent evaporation. A precursor of a bridged silsesquioxane based on the reaction product of (glycidoxypropyl)trimethoxysilane (2 mol) with dodecylamine (1 mol) was hydrolytically condensed in a THF solution at room temperature in the presence of formic acid, water, and variable amounts of dodecanethiol-stabilized gold NPs (average diameter of 2 nm). The initial compatibility of the precursor with gold NPs was achieved by the presence of dodecyl chains in both components. Phase separation of gold NPs accompanied by partitioning to the air−polymer interface took place driven by the polycondensation reaction and solvent evaporation. A hierarchical organization of gold NPs in the structures generated at the air−polymer interface was observed. Small body-centered cubic (bcc) crystals of about 20 nm diameter were formed in the first step, in which the 2 nm gold NPs kept their individuality (high-resolution transmission electron microscopy, field emission scanning electron microscopy, and small-angle X-ray diffraction). In the second step, bcc crystals aggregated, forming compact micrometer-sized spherical particles. Under particular evaporation rates a third step of the self-assembly process was observed where micrometer-sized particles formed fractal structures. Increasing the initial concentration of gold NPs in the formulation led to more compact fractal structures in agreement with theoretical simulations. The surface percolation of NPs in fractal structures can be the basis of useful applications.

Introduction

The organization of nanoparticles (NPs) into two- and three-dimensional structures leads to materials characterized by different properties compared to those of the individual particles.[1−6] This is due to the collective interactions among the set of particles in the self-assembled domains that leads to novel electrical,[7,8] optical,[9,10] and magnetic[11−14] properties. Strategies that allow the controlled formation of clusters of the desired size and shape in which NPs preserve their individuality can be useful for a high number of applications that take advantage of the collective interactions. Of particular interest is the hierarchical array of clusters of self-assembled NPs into percolating networks either in solution[15] or at the surface of a polymeric film.[16,17] Antistatic coatings with high electrical conductivity and high optical transparency were obtained by generating percolating clusters of antimony-doped tin oxide (ATO) either in thin surface layers[16] or throughout the bulk of the sample.[18] Nanoporous metal superstructures with a narrow size distribution of pores have been produced by hierarchical self-assembly and fusion of gold nanoparticles.[19] Superhydrophobic materials have been successfully obtained by modifying surfaces with fractal and dendritic metal superstructures.[20,21] Silver and gold NP aggregates have demonstrated high activity as surface-enhanced Raman scattering (SERS) substrates.[22]

The self-assembly of nanoparticles stabilized by organic groups in a polymer may be induced using different strategies.[5,6] In a recent study we showed that gold nanoparticles stabilized by

* To whom correspondence should be addressed. E-mail: hoppe@fi.mdp.edu.ar (C.E.H.); williams@fi.mdp.edu.ar (R.J.J.W.).
[†] University of Mar del Plata and CONICET.
[‡] University of Barcelona.
[§] University of Santiago de Compostela.

(1) Alivisatos, A. P. *Science* **1996**, *271*, 933.
(2) Pileni, M. P. *J. Phys. Chem. B* **2001**, *105*, 3358.
(3) Liz-Marzán, L. M., Kamat, P. V., Eds. *Nanoscale Materials*; Kluwer: Boston, 2003.
(4) Pileni, M. P., Ed. *Nanocrystals Forming Mesoscopic Structures*; Wiley-VCH: Weinheim, Germany, 2005.
(5) Shenhar, R.; Norsten, T. B.; Rotello, V. M. *Adv. Mater.* **2005**, *17*, 657.
(6) Vaia, R. A.; Maguire, J. F. *Chem. Mater.* **2007**, *19*, 2736.
(7) Collier, C. P.; Saykally, R. J.; Shiang, J. J.; Henrichs, S. E.; Heath, J. R. *Science* **1997**, *277*, 1978.
(8) Wang, G. R.; Wang, L.; Rendeng, Q.; Wang, J.; Luo, J.; Zhong, C. *J. Mater. Chem.* **2007**, *17*, 457–462.
(9) Srivastava, S.; Frankamp, B. L.; Rotello, V. M. *Chem. Mater.* **2005**, *17*, 487.
(10) Uhlenhaut, D. I.; Smith, P.; Caseri, W. *Adv. Mater.* **2006**, *18*, 1653.
(11) Dormann, J. L.; Fiorani, D.; Tronc, E. *Adv. Chem. Phys.* **1997**, *98*, 283.
(12) El-Hilo, M.; O'Grady, K.; Chantrell, R. W. *J. Magn. Magn. Mater.* **1992**, *114*, 295.
(13) Hoppe, C. E.; Rivadulla, F.; Vidal-Vidal, J.; López-Quintela, M. A.; Rivas, J. J. *Nanosci. Nanotechnol.* **2008**, *8*, 2883.
(14) Hoppe, C. E.; Rivadulla, F.; López-Quintela, M. A.; Buján, M. C.; Rivas, J.; Serantes, D.; Baldomir, D. *J. Phys. Chem. C* **2008**, *112*, 13099.
(15) Hussain, I.; Wang, Z.; Cooper, A. I.; Brust, M. *Langmuir* **2006**, *22*, 2938.
(16) Wakabayashi, A.; Sasakawa, Y.; Dobashi, T.; Yamamoto, T. *Langmuir* **2006**, *22*, 9260.
(17) Zucchi, I. A.; Hoppe, C. E.; Galante, M. J.; Williams, R. J. J.; López-Quintela, M. A.; Matějka, L.; Slouf, M.; Pleštil, J. *Macromolecules* **2008**, *41*, 4895.
(18) Wakabayashi, A.; Sasakawa, Y.; Dobashi, T.; Yamamoto, T. *Langmuir* **2007**, *23*, 7990.
(19) Kim, M.; Jeong, G. H.; Lee, K. Y.; Kwon, K.; Han, S. W. *J. Mater. Chem.* **2008**, *18*, 2208.
(20) Wang, T.; Hu, X.; Dong, S. *Chem. Commun.* **2007**, 1849.
(21) Shi, F.; Wang, Z.; Zhang, X. *Adv. Mater.* **2005**, *17*, 1005.
(22) Baker, G. A.; Moore, D. S. *Anal. Bioanal. Chem.* **2005**, *382*, 1751.

10.1021/la8033403 CCC: $40.75
Published on Web 12/23/2008

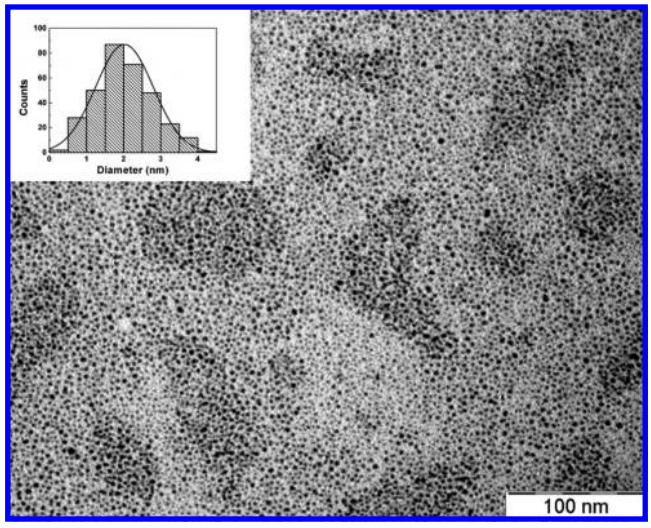

Figure 1. TEM image of the dodecanethiol-coated gold NPs. The inset shows the size distribution of the metallic core of the gold NPs.

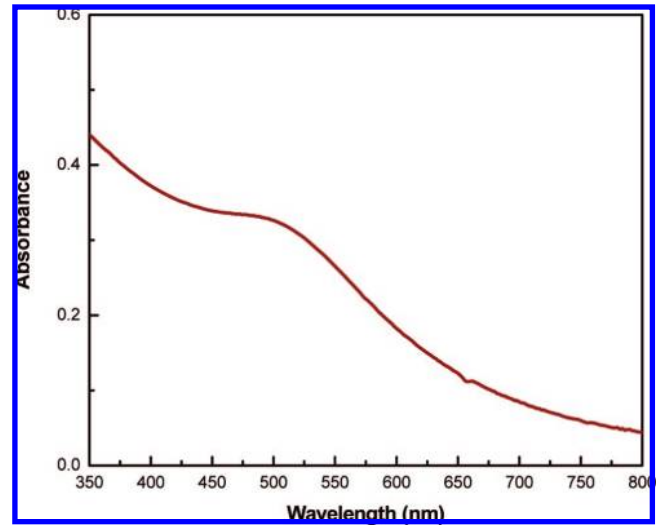

Figure 2. UV−vis spectrum of a dispersion of gold NPs in heptane.

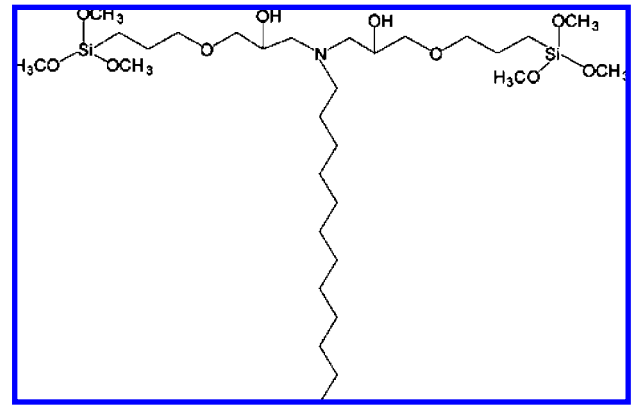

Figure 3. Structure of the precursor of the bridged silsesquioxane.

dodecyl groups could be homogeneously dispersed in precursors of an epoxy polymer based on stoichiometric amounts of diglycidyl ether of bisphenol A and dodecylamine.[17] However, phase separation occurred in the course of polymerization, as predicted by simple thermodynamic models,[23] leading to the self-assembly of gold nanoparticles into colloidal crystals dispersed in the polymer matrix, with a significant partitioning at the air−polymer interface.[17] The relatively high polymerization temperature (100 °C) produced changes in the initial size distribution of nanoparticles (increase in the mean size and narrowing of the size distribution) that enabled the formation of colloidal crystals.

The aim of this study was to investigate the behavior of an initial homogeneous dispersion of gold nanoparticles in a precursor that can polymerize at room temperature to minimize changes in the particle size distribution. The precursor of a bridged silsesquioxane with a pendant dodecyl chain was selected for this purpose.[24] Terminal trimethoxysilyl groups can undergo polycondensation at room temperature in solution by a typical sol−gel reaction. The pendant dodecyl chain can provide initial miscibility for gold nanoparticles stabilized by dodecanethiol chains. In particular, conditions leading to the partitioning of self-assembled clusters of NPs at the air−polymer interface will be analyzed.

Experimental Section

Synthesis of Dodecanethiol-Coated Gold NPs. Dodecanethiol-coated gold NPs were synthesized using a modification of the Brust−Schiffrin method.[25] Briefly, 1.1 mmol of $HAuCl_4 \cdot 3H_2O$ was dissolved in a solution of tetraoctylammonium bromide in toluene. After the resulting solution was stirred overnight, dodecanethiol (DDT) was added in a molar ratio of 0.9 with respect to gold. An excess of freshly prepared sodium borohydride aqueous solution was then added as a reducing agent. The as-synthesized DDT-coated gold NPs were separated from unattached DDT by precipitation with ethanol (in a volume ratio with respect to the toluene solution of 7:1), followed by centrifugation (8000 rpm). The wet product was dried at 40 °C and stored as a waxy solid at room temperature.

Figure 1 shows a TEM image of the dodecanethiol-coated gold NPs. The inset shows the size distribution of the Au cores. The largest fraction of particles was the one with diameters between 1.5 and 2 nm, with an average value of 2.0 nm for the whole population. A UV−vis spectrum of a dispersion of NPs in heptane displaying a weak surface plasmon band envelope around 515 nm is shown in Figure 2. The shape and position of this band agree with results previously reported for gold NPs of similar sizes.[26,27]

Synthesis of Films of the Bridged Silsesquioxane Modified with Gold Nanoparticles. The synthesis of the precursor of the bridged silsesquioxane (Figure 3) was reported elsewhere.[24] The precursor also includes a series of oligomers derived from the condensation of $Si(OCH_3)$ with COH groups. In the course of the sol−gel polycondensation these oligomers are hydrolyzed and contribute to the formation of the bridged silsesquioxane.

A 0.1 M solution of the precursor in tetrahydrofuran (THF) was employed, containing variable amounts of stabilized-gold NPs in a weight ratio varying from 0 to 1 wt % with respect to the precursor. These initial solutions were homogeneous. The sol−gel reaction was performed by adding formic acid and water in molar ratios HCOOH/Si = 0.1 and H_2O/Si = 3. Solutions (25 cm^3) were cast in polyacetal recipients of 5 cm diameter. A glass cover that could be shifted in height was used to control the solvent evaporation rate. Hydrolysis and condensation reactions took place at 18 °C together with solvent evaporation. Free-standing films with a thickness of

(23) Soulé, E. R.; Borrajo, J.; Williams, R. J. J. *Macromolecules* **2007**, *40*, 8082.
(24) Romeo, H. E.; Fanovich, M. A.; Williams, R. J. J.; Matějka, L.; Pleštil, J.; Brus, J. *Macromolecules* **2007**, *40*, 1435.
(25) Brust, M.; Walker, M.; Bethell, D.; Schiffrin, D. J.; Whyman, R. *Chem. Commun.* **1994**, 801.
(26) Hostetler, M. J.; Wingate, J. E.; Zhong, C. J.; Harris, J. E.; Vachet, R. W.; Clark, M. R.; Londono, J. D.; Green, S. J.; Stokes, J. J.; Wignall, G. D.; Glish, G. L.; Porter, M. D.; Evans, N. D.; Murray, R. W. *Langmuir* **1998**, *14*, 17.
(27) Maye, M. M.; Zheng, W.; Leibowitz, F. L.; Ly, N. K.; Zhong, C. J. *Langmuir* **2000**, *16*, 490.

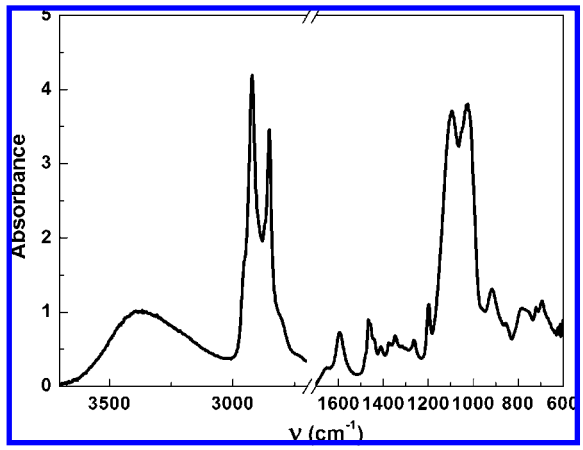

Figure 4. FTIR spectrum of an unmodified film of the bridged silsesquioxane.

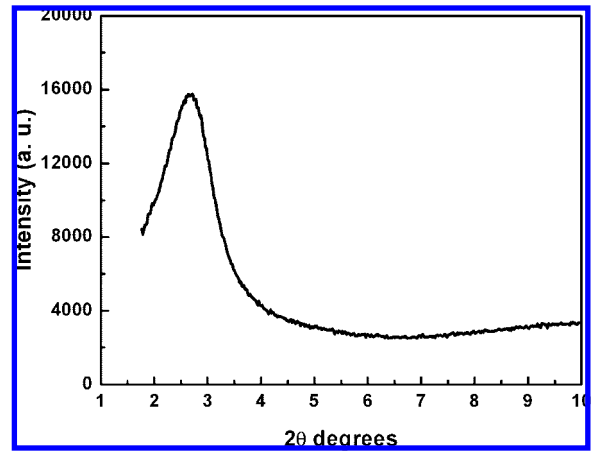

Figure 5. Small-angle X-ray diffraction spectrum of the bridged silsesquioxane.

about 500 μm could be detached from the mold after 1−4 weeks, depending on the solvent evaporation rate. The film without gold NPs was transparent and slightly yellow, while those modified with gold NPs had a color varying from red (0.1 wt % NPs) to brown (1 wt % NPs), with a decreasing transparency.

Characterization Techniques. Fourier-transformed infrared spectra were obtained in the attenuated total reflectance mode (FTIR, Genesis II, Mattson). UV−vis spectra were recorded on a double-beam spectrophotometer, Shimadzu 1601 PC. X-Ray diffraction (XRD) spectra were obtained with a Philips PW1710 or a Siemens D5005 powder diffractometer in grazing incidence mode using Cu Kα radiation.

The size distribution of as-synthesized gold NPs was determined using a Philips CM-12 transmission electron microscope operated at an accelerating voltage of 100 kV. Samples were prepared by dropping 6 μL of a dispersion of the particles on a copper grid coated with Formvar and a carbon film.

Hierarchical structures of self-assembled gold NPs were observed using a set of optical and electron microscopes. Transmission optical microscopy (TOM) images were taken with a Leica DMLB microscope provided with a video camera (Leica DC100). Scanning electron microscopy (SEM) images were obtained using a Zeiss DSM 982 Gemini FEG-SEM microscope, an FESEM Zeiss Supra 40, and a Jeol JSM-6460LV device provided with an EDAX analyzer system (Genesis Spectrum V5.11). Transmission electron microscopy (TEM) images of ultrathin sections were obtained with a Jeol JEM-2010 FEG microscope.

To attain topographical information of the film surface, optical images and surface profiles were acquired with a Zygo New View 100 scanning white light interferometer microscope.

Results and Discussion

Neat Films of the Bridged Silsesquioxane. In the presence of an acid catalyst and water, terminal Si(OCH_3) groups of the precursor are converted into Si(OH) groups that react among themselves or with Si(OCH_3) groups, leading to a cross-linked polymer through the formation of Si−O−Si bonds. The bridged silsesquioxane undergoes a nanostructuration process during which organic bridges become self-assembled through dodecyl−dodecyl interactions.[24] Figure 4 shows an FTIR spectrum of the unmodified film. The presence of the two peaks at 1020 and 1090 cm^{-1} is characteristic of antisymmetric Si−O−Si vibrations. These peaks are located at relatively low frequencies when compared with those found for a similar product exhibiting a high conversion in the polycondsensation reaction (in this case peaks were present at 1040 and 1118 cm^{-1}).[24] This indicates a relatively low conversion in the polycondensation reaction, a fact that is corroborated by the presence of a relatively intense peak at 916 cm^{-1}, assigned to SiOH groups. The broad band with a maximum at 3370 cm^{-1} is characteristic of H-bonded SiOH and COH groups. The two peaks at 2850 and 2920 cm^{-1} are characteristic stretching vibrations of CH_2 groups in extended chains (all-trans conformation).[28]

A small-angle X-ray diffraction spectrum of the unmodified film is shown in Figure 5. The broad peak with a maximum at $2\theta = 2.686°$ corresponds to a scattering vector $q = (4\pi/\lambda) \sin \theta = 0.191$ $Å^{-1}$ or a length $d = 2\pi/q = 32.9$ Å. This is the characteristic distance of tail-to-tail associations of extended dodecyl chains, as reported in a previous paper.[24] The broadness of the peak indicates that the nanostructuration of the bridged silsesquioxane exhibits a short-range order. A correlation length (ζ) related to the structural order range associated with this peak may be defined as[29]

$$\zeta = 2\pi/\Delta q$$

where Δq is the full width at half-maximum measured in units of the scattering vector. The calculated correlation length is $\zeta = 65$ Å, meaning that on the average the ordering extends over a distance that is twice the characteristic length.

Influence of the Solvent Evaporation Rate on Structures Generated at the Air−Polymer Interface in Films Modified with Gold NPs. The nature of superlattices formed by solvent evaporation during drop-casting solutions of gold NPs depends on the solvent evaporation rate. A rapid evaporation generates a fast-moving liquid−air interface compared to the diffusion of nanoparticles, leading to the trapping of NPs at the interface, generating highly ordered 2D structures.[30,31] At low evaporation rates, NPs can diffuse away from the interface at a faster rate than the moving boundary. When the concentration attains a critical value, nucleation of 3D structures takes place.[32] Film formation in our case was carried out at low evaporation rates, and the critical concentration of NPs was attained by both solvent evaporation (increases the concentration of NPs) and sol−gel polymerization (decreases the solvent quality). Two sets of films were obtained by adjusting the evaporation rate to obtain self-standing detachable films in 2 weeks (standard conditions) or in 4 weeks (low evaporation rates). Significant differences in the

(28) Wang, R.; Baran, G.; Wunder, S. L. *Langmuir* **2000**, *16*, 6298.
(29) Moreau, J. J. E.; Vellutini, L.; Dieudonné, P.; Wong Chi Man, M.; Bantignies, J. L.; Sauvajol, J. L.; Bied, C. *J. Mater. Chem.* **2005**, *15*, 4943.
(30) Bigioni, T. P.; Lin, X. M.; Nguyen, T. T.; Corwin, E. I.; Witten, T. A.; Jaeger, H. M. *Nat. Mater.* **2006**, *5*, 265.
(31) Narayanan, S.; Wang, J.; Lin, X. M. *Phys. Rev. Lett.* **2004**, *93*, 135503.
(32) Constantinides, M. G.; Jaeger, H. M.; Li, X.; Wang, J.; Lin, X. M. *Z. Kristallogr.* **2007**, *222*, 595.

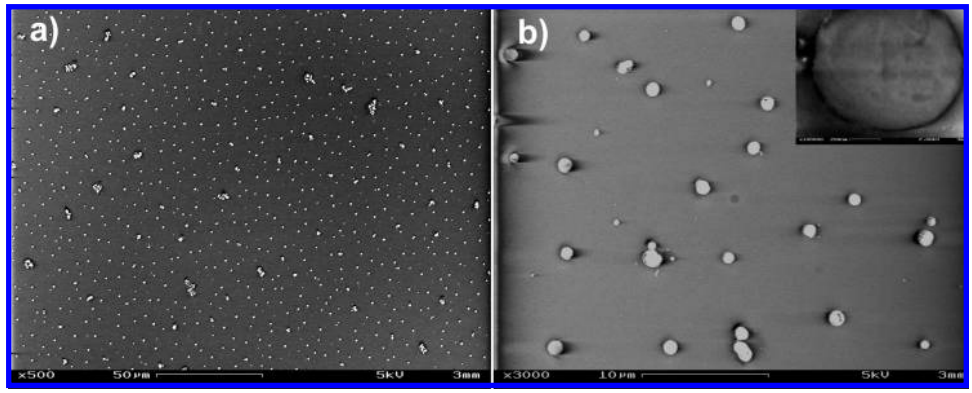

Figure 6. SEM micrographs of the surface of a film containing 0.7% gold NPs obtained with a low evaporation rate. (a) and (b) are different magnifications. The inset in (b) shows a high-resolution SEM image of one of the large particles.

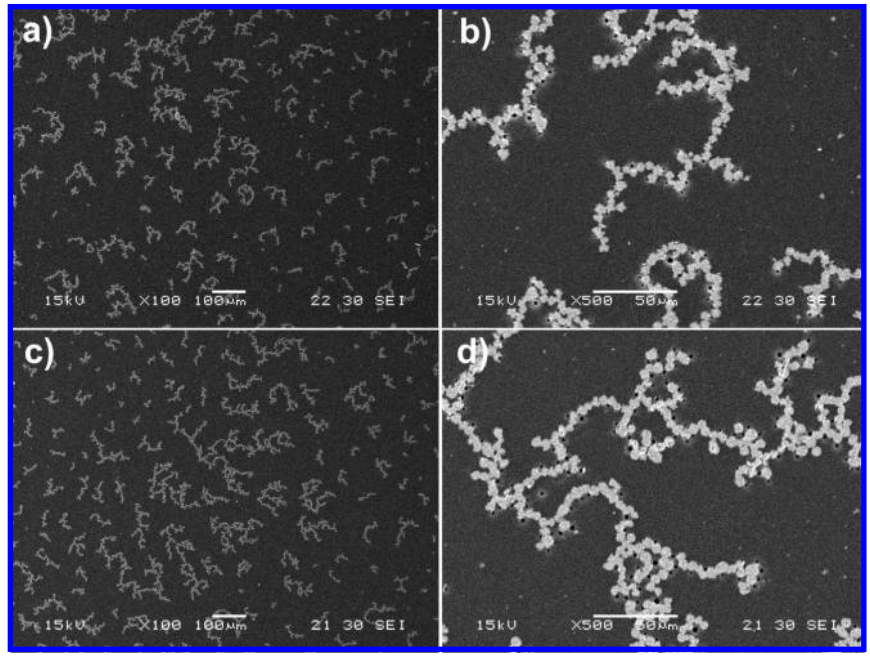

Figure 7. SEM micrographs of the surface of films obtained at standard conditions. (a) and (b) are different magnifications of a film with 0.3 wt % gold NPs, and (c) and (d) are different magnifications of a film with 0.5 wt % gold NPs.

partitioning and organization of gold NPs at the air−polymer interface were observed in both cases.

Figure 6 shows SEM images of the surface of a film containing 0.7% gold NPs obtained with a low evaporation rate. A uniform distribution of spherical particles with diameters close to 1 μm is present at the film surface. Aggregates of particles are observed in some regions as well as the presence of smaller particles with sizes in the 0.1−1 μm range. The inset of Figure 6b shows an individual 1 μm particle. EDAX confirmed the presence of gold inside dispersed particles.

The situation changed completely for films obtained at standard conditions as shown in Figure 7. Fractal structures formed by the aggregation of quasi-spherical particles were generated at the surface of the films together with a dispersion of individual smaller particles. The average size of the particles was close to 5 μm for the formulation containing 0.3 wt % NPs and 8 μm for the formulation containing 0.5 wt % NPs.

These experimental results prove that the partitioning of gold NPs to the surface of the films exhibits a significant dependence on the solvent evaporation rate. Increasing this rate produced an increase in the size of particles as well as their aggregation into fractal structures at the air−polymer interface. Reasons for this behavior will be discussed after the next section.

Figure 8 shows the morphology generated for a film containing 1 wt % gold NPs obtained at standard conditions. Fractal structures formed by 10 μm spherical particles covering an area of about 1 mm^2 can be observed. A white light interferometry micrograph for a film containing 0.7 wt % gold NPs obtained at standard conditions shows that these micrometric particles protrude about 0.5 μm from the flat surface of the polymeric film (Figure 9). It is interesting to note that fractal structures obtained at these higher concentrations look more compact than those shown in Figure 7.

Hierarchical Organization of Gold NPs inside Large Particles. In this section the eventual coalescence and/or crystallization of individual gold NPs inside large particles will be examined. Due to the small size of individual gold NPs, small-angle X-ray diffraction could be used (instead of small-angle X-ray scattering, SAXS) to assess the eventual formation of a crystalline self-assembly. Figure 10 shows a small-angle X-ray diffraction spectrum for a material containing 0.7 wt % gold NPs synthesized at standard conditions. The asymmetric peak present

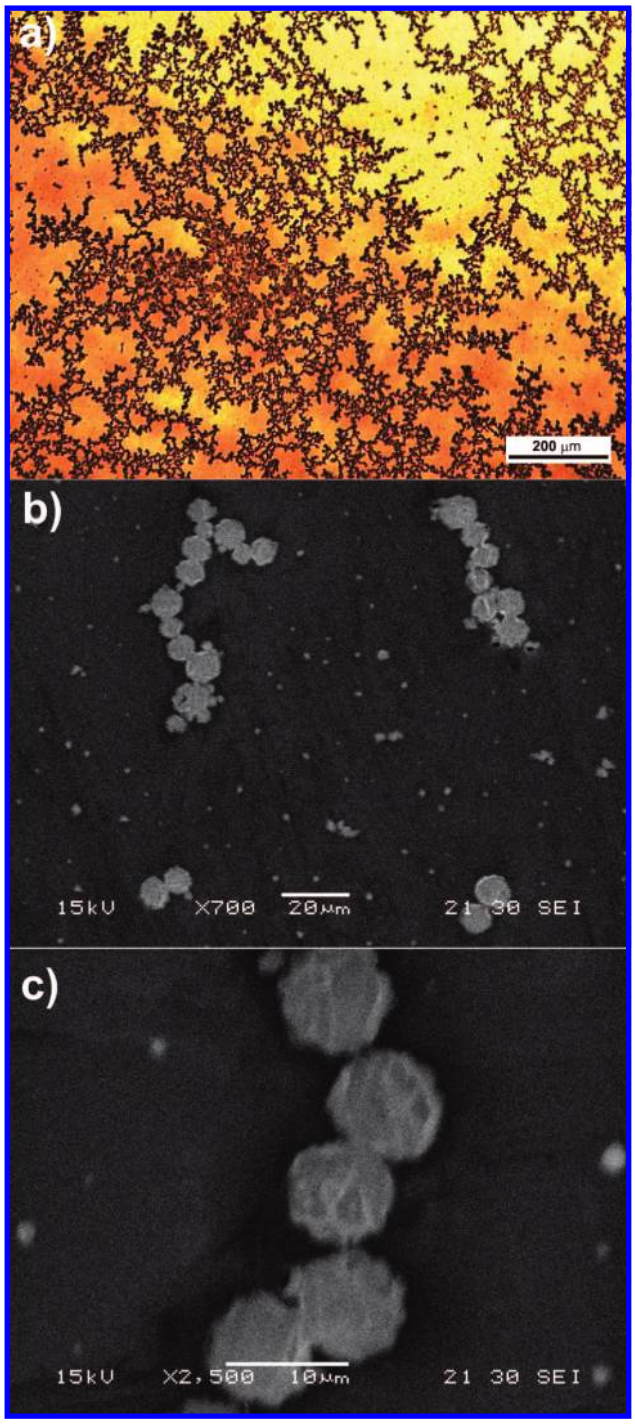

Figure 8. SEM micrographs of the surface of a film containing 1 wt % gold NPs obtained at standard conditions. (a) is a TOM image, and (b) and (c) are SEM images at different magnifications.

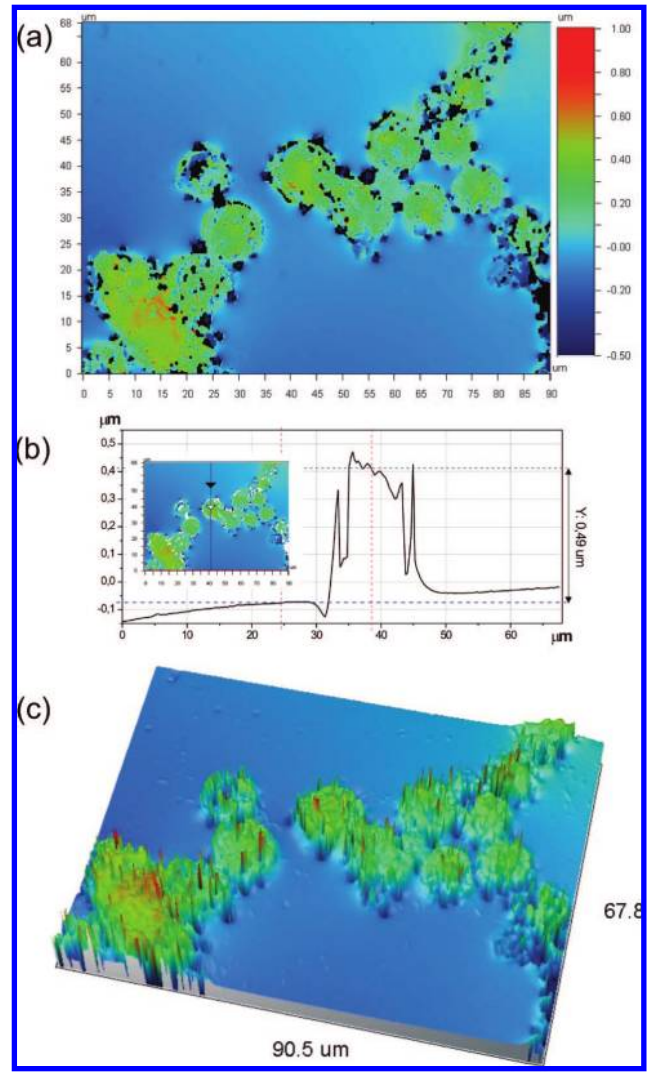

Figure 9. Microscopic surface structure acquired by scanning white light interferometry of a film containing 0.7 wt % gold NPs obtained at standard conditions: (a) 2D image, (b) *y*-profile, and (c) 3D image.

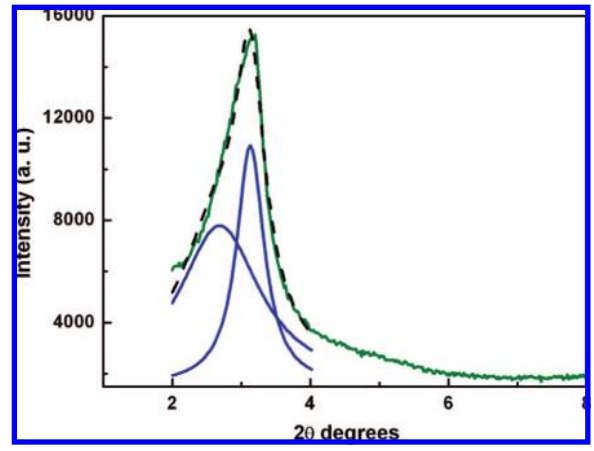

Figure 10. Small-angle X-ray diffraction spectrum for a material containing 0.7 wt % gold NPs synthesized at standard conditions.

at low angles could be deconvoluted into two Lorentzian peaks: one broad peak with a maximum at $2\theta = 2.686°$ and a narrower peak with a maximum at $2\theta = 3.126°$. The former is located at exactly the same position as the peak present in the matrix and may be therefore assigned to the tail-to-tail association of dodecyl chains of the bridged silsesquioxane.

The presence of a second diffraction peak at $2\theta = 3.126°$ reflects a local order (crystallinity) in the self-assembly of gold NPs. Crystal structures formed by gold NPs coated with *n*-alkyl ligands were analyzed by Whetten at al.[33] They observed that the crystal structure depends exclusively on the value of the parameter $\chi = 2L/D_{core}$, where L is the thickness of the corona equated to the fully extended (all-trans) chain length ($L = 1.6$ nm for dodecyl chains) and D_{core} is the diameter of the gold-nanocrystal core. Therefore, in our case $\chi = 2(1.6\text{ nm})/(2\text{ nm}) = 1.6$. For this value of χ the expected crystal structure is a

body-centered cubic (bcc) structure. Eventually, some lower symmetry structure might be generated such as the body-centered tetragonal (bct) structure with 15% elongation along one axis.[33] Another significant observation reported in that paper is the high packing efficiency of the corona in the crystal structure. For the case of dodecyl chains, the edge-to-edge distance of the gold cores of two neighboring particles is located in the range of 1.6−1.7 nm, independently of the core size and the corresponding crystal structure.[33] This distance is about half the expected value for a bilayer of extended chains, implying a chain-packing density corresponding to the solid-crystalline alkane phase.

Assuming that the scattering peak at $2\theta = 3.126°$ can be assigned to the first allowed reflection (110) of the bcc structure, the center-to-center distance between neighboring particles (D_{nn}) may be calculated as $D_{nn} = (3/2)^{1/2}\lambda/(2 \sin \theta)$,[33] where $\lambda = 0.154$ nm is the wavelength of the Cu Kα radiation. This gives $D_{nn} =$ 3.46 nm. Discounting the edge-to-edge distance of the cores, estimated as 1.65 nm,[33] leads to a core diameter of 1.8 nm, which is in the range of the most frequent particles present in the experimental size distribution (inset of Figure 1). Therefore, we may conclude that gold NPs are primarily organized into bcc crystals although lower symmetry structures cannot be discarded. The value of the correlation length is $\zeta = 18.2$ nm, implying the presence of small crystalline regions (either small crystals or local organization in larger agglomerates of gold NPs).

The eventual presence of isolated crystals in the films was searched by field emission scanning electron microscopy (FESEM) and high-resolution transmission electron microscopy (HRTEM). Figure 11a is a FESEM image of the film surface showing the presence of aggregates of individual NPs with typical sizes in the 10−30 nm range, which is on the order of the correlation length found for the X-ray scattering peak. HRTEM images obtained from the bulk of the films obtained under slow evaporation rates (Figure 11b,c) also show the presence of a low concentration of NP aggregates. These clusters of NPs show, on average, a lower size and organization level than those observed at the surface of the film and probably represent an intermediate step (frozen by gelation) in the formation of bcc crystals. Therefore, we may infer that the first step in the self-assembly of the 2 nm NPs is the formation of bcc crystals with a mean size in the range of 20 nm.

As individual NPs present in the aggregates shown in Figure 11 kept their initial size, we can conclude that their coalescence did not occur under the selected polymerization conditions. This fact was corroborated by the UV−vis spectra of films containing different amounts of gold NPs, obtained at standard conditions (Figure 12). Constancy in the location of the plasmon peak with respect to that shown by dispersions of initial gold NPs in heptane (Figure 2) reassures that coalescence did not take place. The small increase of the absorbance at long wavelengths is consistent with particle−particle interactions associated with the formation of aggregates.[15] Similar UV−vis spectra were observed for films synthesized with low evaporation rates.

Most micrometric particles present at the film surface exhibited a compact skin assigned to a thin layer of silsesquioxane that encapsulates the contents (e.g., see the inset of Figure 6b). A few particles appeared partially broken, exhibiting their interior. Figure 13 shows an FESEM image of one such particle (diameter close to 1.5 μm), present at the surface of a film with 0.7 wt % gold NPs. The interior is formed by the agglomeration of spherical aggregates with sizes in the range of 20−30 nm. Therefore, it may be inferred that large particles are formed by aggregation

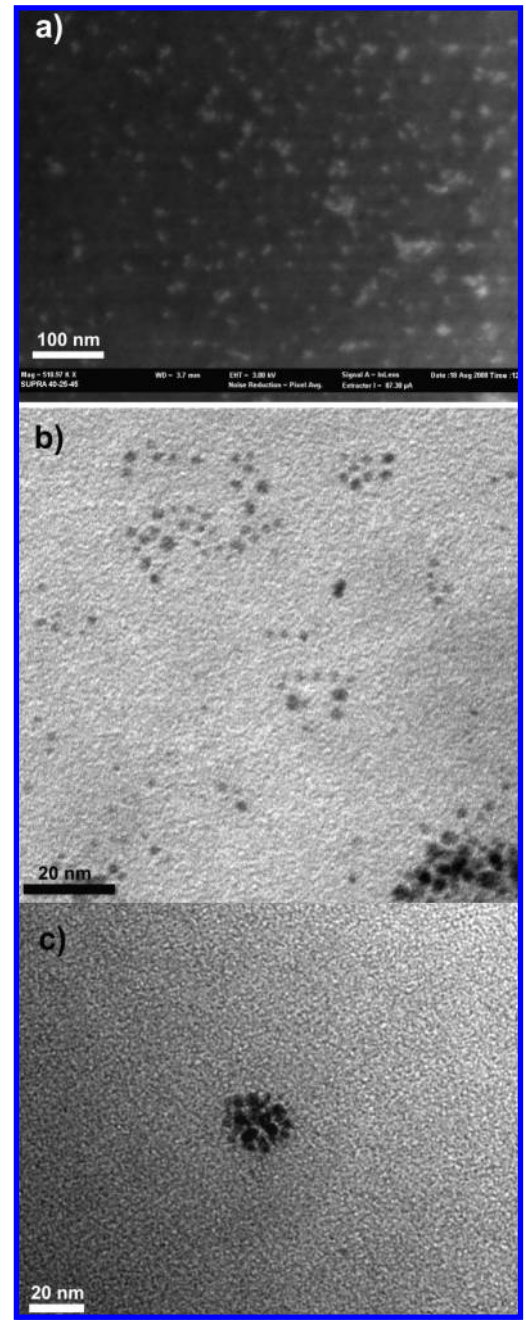

Figure 11. (a) High-resolution SEM image showing the presence of small NP aggregates at the surface of the film. (b, c) HRTEM images obtained from ultrathin cuts of a film containing 0.11% gold NPs obtained with a low evaporation rate.

of bcc crystals with diameters in the range of 20−30 nm. To complete the picture of the hierarchical organization, we intended to assess the presence of the individual 2 nm NPs inside the crystals forming the large particles. High-resolution SEM images were obtained from the interior of one of the partially broken particles. Although these images were obtained at the limit of resolution of the device, they supported the presence of individual 2 nm NPs inside the micrometer-sized particles (Figure 14).

Discussion of the Hierarchical Organization of Gold NPs. An explanation of the sequence of events leading to the hierarchical organization of gold NPs may be proposed. In the initial system constituted by the precursor of the bridged silsesquioxane, gold NPs, and a solvent (THF), the NPs were individually dispersed. During the process of film formation, the continuous solvent evaporation generated a gradient in solvent

(33) Whetten, R. L.; Shafigullin, M. N.; Khoury, J. T.; Schaaff, T. G.; Vezmar, I.; Alvarez, M. M.; Wilkinson, A. *Acc. Chem. Res.* **1999**, *32*, 397.

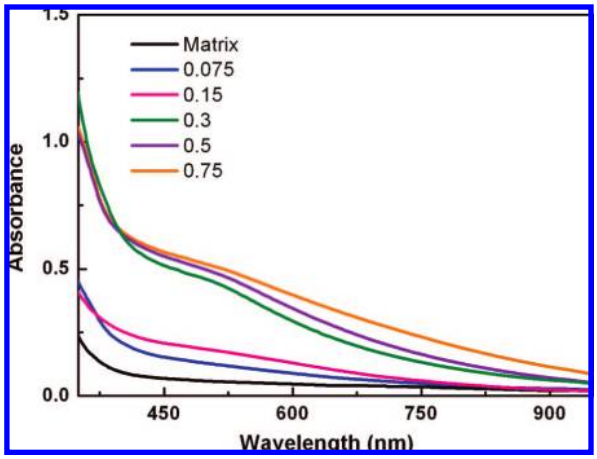

Figure 12. UV−vis spectra of films containing different concentrations (wt %) of gold NPs obtained at standard conditions.

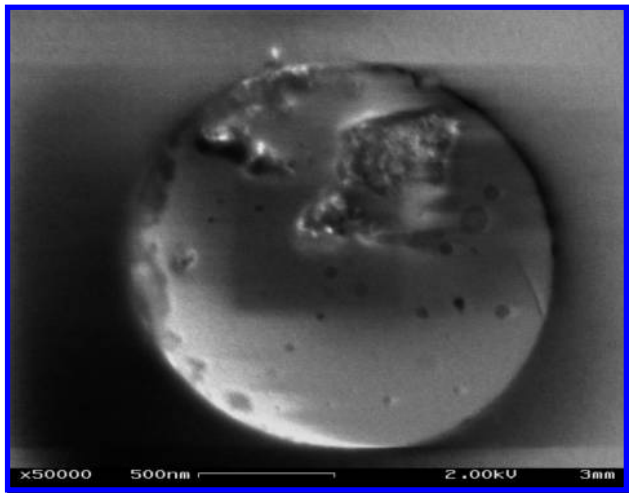

Figure 13. FESEM image of a partially broken particle present at the surface of a film containing 0.7 wt % gold NPs.

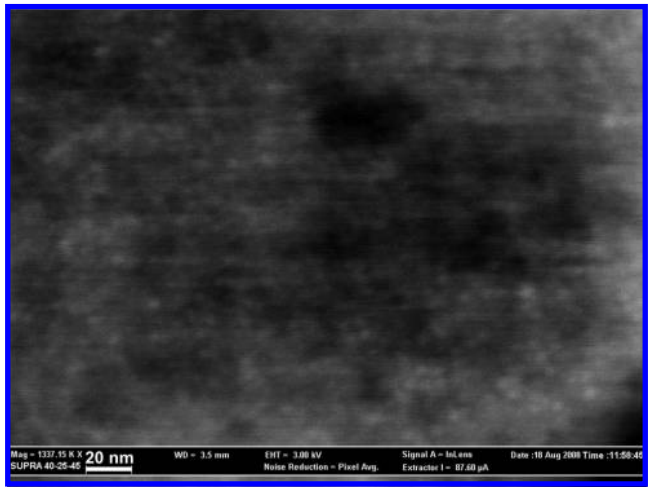

Figure 14. High-resolution SEM image showing the interior of a partially broken particle.

concentration with the lowest concentration at the film surface. This was accompanied by a corresponding increase in the concentration of species undergoing polymerization, with higher conversions close to the film surface. At a particular point during this process NPs attained the critical concentration necessary to phase-separate from the solution. Supersaturation was the consequence of solvent evaporation and the increase in size of the oligomers generated in the sol−gel reaction.[23] Therefore, the gradient in solvent concentration produced phase separation at the film surface.

The presence of a gradient in solvent concentration generates a flux of solvent from the bottom to the surface of the film. Thermal gradients originated by the heat of vaporization can also contribute to the convective flux of solvent.[16] NPs still dispersed in the bulk of the solution were transported to the surface where they became phase separated, increasing the concentration of stable structures. This produced the partitioning of gold NPs along the film thickness. The process is evaporation-driven and is referred to as convective assembly of NPs.[34−37] The partitioning of gold NPs at the surface of the polymer film should increase with the solvent evaporation rate due to the generation of a steeper gradient of solvent concentration. This agrees with the experimental findings (compare Figures 6 and 7).

The first step of the phase separation process was the formation of small bcc colloidal crystals with a mean size in the 20 nm range, detected by small-angle X-ray diffraction and observed by HRTEM and high-resolution SEM. Due to the small van der Waals forces associated with 2 nm NPs, larger crystals were not produced. Instead, small bcc crystals agglomerated, forming the spherical micrometer-sized aggregates observed by TOM and SEM at the air−polymer interface. This hierarchical self-assembly could be induced by a reaction-limited colloid aggregation (RLCA) process[38] taking place between weakly interacting particles. Under these conditions the 20 nm colloidal crystals could be continuously incorporated and removed from the aggregates, finally converging to the compact micrometer-sized quasi-spherical particles present at the air−polymer interface. For low evaporation rates this picture corresponds to the final structure observed at the film surface (Figure 6). For standard evaporation rates a third step of the self-assembly process was observed possibly as a consequence of the increase in the concentration and size of the particles formed during the second step. Now, these large particles formed fractal structures possibly through a diffusion-limited colloid aggregation (DLCA) process.[38−40] This process occurs when there is a negligible repulsive force between the particles and an attractive potential enabling sticking of the particles, so that the aggregation rate is limited by the time taken for clusters to encounter each other by diffusion. Sticking of particles might be induced by the attractive interactions between the polysilsesquioxane layers encapsulating the aggregates. Finally, gelation of the bridged silsesquioxane arrested the growth of the fractal structure.

Depending on the initial concentration of gold NPs in the formulation, qualitative differences in the fractal structures generated at the surface were observed (Figures 6 and 8). For small particle concentrations (Figure 6), the branching level was lower, the branches were thinner, and the structure was less compact (lower fractal dimension), which would indicate that aggregation took place by a diffusion-limited cluster−cluster aggregation mechanism.[40] In the case of higher NP concentrations (Figure 8) formation of more compact structures (higher fractal

(34) Denkov, N. D.; Velev, O. D.; Kralchevsky, P. A.; Ivanov, I. B.; Yoshimura, H.; Nagayama, K. *Langmuir* **1992**, *8*, 3183.
(35) Dimitrov, A. S.; Nagayama, K. *Chem. Phys. Lett.* **1995**, *243*, 462.
(36) Dimitrov, A. S.; Nagayama, K. *Langmuir* **1996**, *12*, 1303.
(37) Prevo, B. G.; Kuncicky, D. M.; Velev, O. D. *Colloids Surf., A* **2007**, *311*, 2.
(38) Lin, M. Y.; Lindsay, H. M.; Weitz, D. A.; Ball, R. C.; Klein, R.; Meakin, P. *Nature* **1989**, *339*, 360.
(39) Witten, T. A.; Sander, L. M. *Phys. Rev. Lett.* **1981**, *47*, 1400.
(40) Meakin, P. *Phys. Rev. Lett.* **1983**, *51*, 1119.

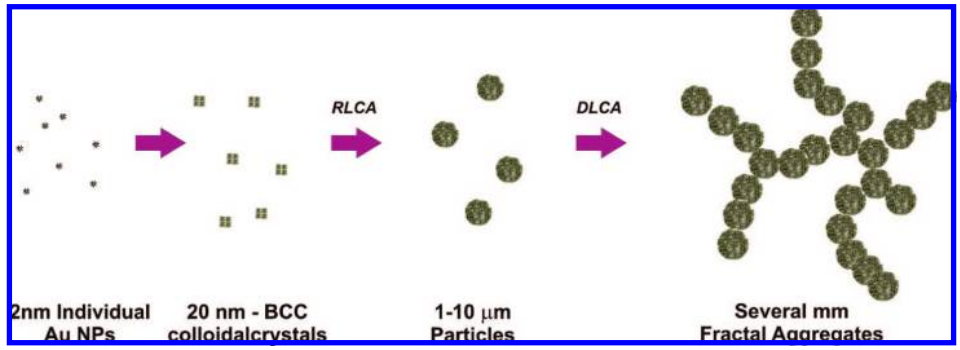

Figure 15. Steps involved in the hierarchical self-assembly process: First, individual gold NPs assembled into small bcc colloidal crystals. In the second step these crystals formed micrometer-sized quasi-spherical aggregates through an RLCA process. Under slow evaporation conditions, gelation precludes further aggregation. For standard evaporation conditions fractal aggregates covering several square milimeters are formed by diffusion, encountering, and sticking of micrometer-sized particles (DLCA).

dimension) suggests a mechanism of diffusion-limited particle−cluster aggregation (Figure 8).[39] These observations agree with predictions from computer simulations of the growth of fractal structures varying the initial concentration of particles.[41] Figure 15 shows a scheme summarizing the different steps involved in the hierarchical self-assembly process.

Conclusions

A THF solution of a precursor of a bridged silsesquioxane containing a pendant dodecyl chain and 2 nm gold NPs stabilized by dodecanethiol chains was used to synthesize free-standing films by polycondensation of the precursor and solvent evaporation. During these processes phase separation of gold NPs was produced, with a significant partitioning at the film surface. A hierarchical organization of gold NPs in the structures generated at the air−polymer interface was observed. Small bcc crystals of about 20 nm diameter were formed in the first step, in which the 2 nm gold NPs kept their individuality. In the second step, bcc crystals aggregated by an RLCA process, forming compact micrometer-sized spherical particles. For low evaporation rates this picture corresponds to the final structure observed at the film surface. For standard evaporation rates a third step of the self-assembly process was observed where particles formed fractal structures through a DLCA process. Increasing the initial concentration of gold NPs in the formulation led to more compact fractal structures in agreement with theoretical simulations.

Solutions of the selected precursor of a bridged silsesquioxane may be used as a host of a variety of nanoparticles stabilized by hydrophobic chains. Controlling the solvent evaporation rate should lead to the generation of fractal structures at the film surface like those observed for dodecanethiol-coated gold NPs. Percolation of these structures, with the subsequent lowering of its threshold, can be the basis of useful applications based on collective optical, magnetic, or transport properties.[2]

Acknowledgment. We acknowledge the financial support of the National Research Council (CONICET, Argentina), the National Agency for the Promotion of Science and Technology (ANPCyT, Argentina, Project PICT06-644), the University of Mar del Plata (Argentina), and the Ministry of Science and Technology (Spain, Projects MAT2005-07554-C02-01 and PGIDIT03PXIC20907PN). C.E.H. gratefully acknowledges the European Commission for financial support (IIF Marie Curie fellowship, Grant MIF2-CT-2006-021689). We thank Marta Otero-Leal for assistance with the XRD measurements.

LA8033403

(41) Beznosyuk, S. A.; Lerh, Y. V.; Zhukovsky, T. M.; Zhukovsky, M. S. *Mater. Sci. Eng., C* **2007**, *27*, 1270.